PARAMETRIC STUDIES ON SEISMIC BEHAVIOR OF FRAME-INFILL SYSTEMS

Ghassan Al-Chaar[1], Daniel P. Abrams[2]

ABSTRACT

This paper summarizes analytical research on stiffness and capacity evaluation of non-ductile reinforced concrete frames with masonry infill panels performed at the US Army Corps of Engineers Construction Engineering Research Laboratory. A series of nonlinear finite element analyses were completed to investigate sensitivities in behavior attributable to various design parameters. Computational simulation models were calibrated with measured data from one-story reinforced concrete frames containing one, two, and three bays. These frames were braced with either masonry or brick infill. The infill-frame structures were constructed at half-scale and subjected to lateral in-plane displacements. Modeling procedures and computed results from this investigation are summarized in this paper.

Finite element models can be employed to supplement expensive testing of large physical models provided that proper simulation exists. Once results of experimental and computational simulations are calibrated, analyses of a large array of different building configurations can be done to investigate plausible concepts for design, evaluation or rehabilitation of actual structures. Research described in this paper addresses variables significant to the determination of ultimate strength and deformation capacities for concrete frames with solid infills, and their sensitivities to variations in material properties and configuration. As well, results of this series of analyses address important variables found in laboratory tests of infill-frame systems, such as mortar type, infill type, load application points, and load distribution.

Key words: Masonry infill, non-ductile reinforced concrete frames, capacity evaluation, in-plane capacity, multi-story buildings, multi-bay buildings, reduction in shear capacity due to openings, experimental and finite element study.

[1] Research Structural Engineer, USAERDC, P.O. Box 9005
Champaign, Illinois 61826-9005
g-al-chaar@cecer.army.mil

[2] Hanson Engineers Professor of Civil Engineering
University of Illinois at Urbana-Champaign
1245 Newmark Civil Engineering Laboratory, 205 North Mathews Avenue
Urbana, Illinois 61801
d-abrams@uiuc.edu

DESCRIPTION OF EXPERIMENTAL MODELS

All test specimens used in this study consisted of a single story of single, double, or triple bay construction. One bare frame and four frames fully infilled were loaded monotonically to a maximum horizontal displacement of 127 to 152.4 mm (8.3%-10% drift). These tests were designed to study each specimen's load-deformation behavior with respect to yield deformation (i.e., up to the appearance of the first crack), ultimate strength, and residual strength under significant drift.

The design of all concrete frames was based on a prototypical structure of a typical dormitory at Castle Air Force Base, California. The building is a three-story reinforced concrete frame constructed in 1952. Its longitudinal frames were the basis for the specimen models. The prototype structures were constructed in accordance with ACI 318-51. Features distinguishing them from newer structures are:

- larger spacing distances between beam stirrups and column ties
- discontinuity in the bottom longitudinal reinforcement of the beam at the joints
- lower steel grade (40 ksi, 276 MPa)
- lower concrete compressive strength
- less stringent code requirements on reinforcement lap splice length and standard hooks
- placement of column reinforcement lap splices directly above floor slab.

Each half-scale model had a total height, from the bottom of the column to the top of the beam, of 1524 mm. Typical bay width was 1829 mm between column centerlines. Columns were 203 mm wide by 127 mm deep; a typical beam was 197 mm deep by 127 mm wide. Prototype and model parameters are shown in Table 1.

Table 1. Prototype and Model Parameters.

Parameter	Prototype	Model
Bay width	160 in. (406.4 cm)	80 in. (203.2 cm)
Bay height	120 in. (304.8 cm)	60 in. (152.4 cm)
Column depth	16 in. (40.6 cm)	8 in. (20.3 cm)
Column width	10 in. (25.4 cm)	5 in. (12.7 cm)
Beam depth	15.5 in. (39.4 cm)	7.75 in. (19.69 cm)
Beam width	10 in. (25.4 cm)	5 in. (12.7 cm)
Column longitudinal reinforcement	4-#6 (ρ=0.0125)	4-#3 (ρ=0.0125)
Column ties	# 3 at 12 in. (30.5 cm) (ρ=0.0065)	6 gage at 6 in. (15.24 cm) (ρ=0.0065)
Beam longitudinal reinforcement	4-#6 top (ρ=0.012) 2-#6 bottom (ρ=0.006)	3-#3 top (ρ=0.012) 2-#3 bottom (ρ=0.0125)
Beam ties	9-#3 at 6 in. (15.2 cm) (ρ=0.013)	6 gage at 3 in. (7.6 cm) (ρ=0.013)

Half-scale 57 mm x 63.5 mm x 127 mm bricks were cut from 102 mm x 63.5 mm x 203 mm standard brick units. Half-scale 102 mm x 102 mm x 279 mm concrete masonry

units were cut from 102 mm x 203 mm x 406 mm standard concrete masonry units. In scaling the dimensions, special emphasis was given to the width and height of the units, not their length. The length was chosen to suit existing holes of the standard masonry units used to cut scaled units from. Concrete and brick wall panels were constructed in a running bond pattern with type N mortar used in all cases. These frames had a slenderness ratio (h_{wall}/t_{wall}) of 13.9 for the CMU wall and 23.13 for the brick wall. The aspect ratios (h_{wall}/l_{wall}) were 1.38 for all walls.

In-plane monotonic loading, stroke-controlled push-over tests were carried out to understand the post-elastic behavior of each model configuration as it was subjected to increasing drift ratios. The specimens were monotonically loaded to a maximum drift of approximately 10%, at a quasi-steady rate of 0.0422 mm per second.

The experimental program consisted of five models. Model 1 was a bare frame non-ductile reinforced concrete frame. Model 2 was a one-bay R/C frame with CMU infill wall. Model 3 was similar to Model 2 except it had a brick infill wall. Model 4 was a two-bay frame with CMU infill, and Model 5 was a three-bay frame with brick infill. Mechanical properties of materials that characterize the experimental models are summarized in Table 2.

DESCRIPTION OF FINITE ELEMENT MODELS

Finite element analyses were carried out for 25 models. In summary, 7 models were half-scale and 18 models were full-scale. Five of the half-scale models were performed for calibration with the experimental results; the full-scale finite element analyses were performed to account for specific variables such as the effect of out-of-plane loading on the in-plane capacity, and load applications. Two full-scale finite element base-models, one for brick infill and one for CMU infill, were designed to be triple-bay triple-story. Three stories were chosen because typical dormitory structures are three stories, and three bays were chosen so the model would consist of all combinations of bay confinements (corner, exterior, and center panels). The geometry and loading of the single-bay single-story models are shown in Figure 1. The base is fixed in all directions at the bottom. The actuator force is applied as a distributed load on one end of the beam for all models except two that were intended to study the difference in the capacity of the base models under one end-point load and several joint-point loads at each floor.

All models were created and executed using the ANSYS program (1998). The various configurations of bare and infilled reinforced concrete frames were subjected to in-plane loading until structural failure occurred. The analyses used non-linear material behavior for all the real physical components. The reinforcing bars included elastic-plastic material behavior. Note the reinforcing bars are included explicitly in the model, and not averaged across a section of the frame. The concrete, mortar, CMU infill, and brick infill elements used material failure surfaces that accounted for material tensile failure and compressive material crushing. The material behavior also included shear transfer for cracked material.

Properties Used in Finite Element Models

There are many components and materials involved in the structures being studied. Table 1 gives the nominal frame dimensions for the half-scale and full-scale models and reinforcing bar properties and sizes used in the analyses. Concrete, mortar, and infill mechanical properties are listed in Table 2. Even though this is a highly non-linear problem, small strain theory was used in the analyses. This was a source for small errors that can be accepted considering the complexity of the system.

A nominal mortar thickness of 10 mm was used. Note that a stack bond was used as an approximation to the running bond. This was used in order to reduce, as much as possible, the total number of elements in the infilled models. All infill patterns were actually separate from the frame. The nodes along the interface were connected using constraint equations. For each model, the mortar nodes associated with the infill at the mortar to frame interface were constrained to displace along the surface defined by the frame nodes.

Loading Types Used in the Analysis

1. In-plane (IP): This loading type consisted of either concentrated in-plane (CIP) loading or distributed in-plane (DIP) loading. CIP loading was concentrated at the beam ends and not applied throughout the structure. This type of loading was used for models 1 through 19. The DIP loading was distributed throughout the bay and story joints of structure at the intersections of the beams and columns. The load was actually applied as a body force using the element volumes at the beam-column intersections. The fixed boundary conditions were chosen so that the models were fixed in all directions at the base.
2. Out-of-plane (OP): This load type was applied as a uniform pressure load to the infill and mortar elements in models 20 and 22. The displacement under this type of loading was monitored at two locations, at the intersection of the beam and column and at the center of the beam. The displacement used is the average of all the displacements in the volume at the beam-column intersections and the average of all the nodes on the center planes of the beams. The relevant displacement for this case was the out-of-plane displacement.
3. Combined OP and CIP loading: This loading type was applied in the following fashion. The OP load to cause failure was found. A new analysis was performed in which ½ of the OP load to cause failure was applied. Then the in-plane load was increased until the structure fails. Since this was a nonlinear analysis, path dependence was important. A precise load history for each loading direction is needed to define the failure history for a particular case. However, this simple loading definition allowed the examination of the interesting questions – how did the in-plane and out-of-plane loading interact and what was the effect on the ultimate load? The in-plane displacement on the plane of CIP loading was used in the load deflection plots.

INTERPRETATION OF RESULTS AND COMPARISON OF EXPERIMENTAL AND FE ANALYSES

Experimental Versus Finite Element Results

Load-deflection curves for experimental and analytical results of the half-scale single-story models are shown in Figures 3 and 4, for the CMU and brick, respectively. Load-deflection curves of single and double bay CMU infilled frames are shown in Figure 3, while single-bay and triple-bay brick infilled frames are presented in Figure 4. Both figures show the load-deflection curves of single-bay bare frame for comparison.

The accuracy of determining the ultimate load depended on the assumed shear retention values that account for shear transfer coefficients for open and closed cracks. Considering the amount of failed material observed in many cases, either the reinforcing bars were very effective in holding the structure together, or the shear retention factor was too high. If these analyses predicted the ultimate load well, then the reinforcing bars were effective in holding the structure together. If these analyses predicted an ultimate load that was higher than experimental values, then the assumed shear retention values may have been too high.

The closeness of the ratios of experimental loads over finite element analysis loads to 1.0 gives an indication of the level of agreement between experimental and analytical procedures. For the single-bay bare frame model the experiment/model ratio was 1.053. The single-bay CMU infilled model had a ratio of 0.82. The brick infilled single-bay model was 0.83. Next was the CMU infilled double-bay frame with a ratio of 1.082. At last, the triple-bay brick infilled frame had a ratio of 1.239.

What these ratios indicate is that the experimental and analytical results agreed within $\pm$20%. Considering the complexity of the problem, such error is reasonable, due to the numerous variables and assumptions in analytical and experimental modeling. It is noted that in the cases of single-bay CMU and the single-bay brick infilled frames, two values of shear retention were examined. Case one, shear retention values in tension and compression of $\beta c=0.6$ and $\beta t=0.3$ were assumed to be consistent with the double and triple bay models. This case yielded higher load capacities than experimental models. Case two, lower shear retention values of $\beta t=\beta c=0.005$ were used for single-bay models, since the reinforcing bars in these models were assumed to be less effective in resisting shear than for the multi-bay models. This case resulted in closer predicted values than were obtained in case one. Case two was believed to be more realistic and can be justified simply because the frames in the single-bay cases provided less friction in the opened cracks and were less effective than the double and triple-bays in binding the structure.

Mortar Type Effect on Triple-Story Triple-Bay Models

The triple-bay, triple-story CMU and brick infill models were analyzed with a stronger mortar, mortar M (1.0 part Portland cement, 0.5 part lime, and 3.5 part sand by volume). The mortar used in the initial work is called mortar N (1.0 part Portland cement, 1.0 part lime, and 6.0 part sand by volume).

The frame with brick infill appeared to be more ductile than the frame with CMU infill, even though the CMU masonry units were stronger. This was attributed to a greater volume of mortar in the brick infill model than in the CMU infill model because the size of the brick unit was smaller than the concrete block unit.

Changing to a stronger mortar affected the load-deflection relationship for similarly loaded and infilled structures. The ultimate load was also increased due to the increased mortar strength. Furthermore, the failed material maps, not illustrated here, showed that for model 18 there were broken CMU blocks. For model 16 there were none. The strength of mortar M and CMU were the same. The failure of mortar and CMU happened at the same load. Initially, the small, very confined volumes of mortar failed. Then the CMU took some of the load and failed. When the CMU failed but the frame can still take significant load, the very large CMU block failures acted as linked up cracks and lowered the stiffness. This was not the case for the bricks that had a much greater failure strength than the CMU.

This was a very important principle in the failure scenario. In models 16 and 17, the failure loads for the 4 materials were widely separated. Loosely speaking, the order of failure was mortar, CMU/concrete/brick, reinforcing bar. However, with the change to the stronger mortar, the CMU failed in cases where it would not have previously failed as the mortar shed its load.

For all of the infill analyses, a substantial amount of mortar failed before any other part of the structure had cracked. Very few of the CMU or bricks failed prior to ultimate, even though the material properties were lower than the concrete. (Except the brick crushing strength.) This was because they were shielded from the bending loading. They were confined inside the columns and beams. In addition the load was running through the mortar that was continually softening, but the load had to pass through the intact mortar that in turn also failed.

The strength increase in the frames by the use of mortar type M is represented in the following ultimate load ratios in triple-story, triple-bay frames. The use of M mortar for the CMU and brick infilled frames resulted in load increases of 10.8% and 14.3% more than the N mortar case, respectively. The ultimate loads in the case of M mortar occurred at higher displacement and higher stiffness values.

With the goal to closely simulate the physical models analytically, it was necessary to pay close attention to provide a precise value for the mortar property used in the models. This may call to rethink current practice where mortar is the least quality-controlled material.

Effects of Out-of-Plane Loading on In-Plane Strength

Out-of-plane loading – In all analyses reported above, loading was in the plane of the frame. This is not realistic, but it was easier to model and understand some fundamental results. Nonlinear loadings are path dependent. For the problems studied here, the path dependence comes about due to the failure of material in a particular loading direction. The failure of a reinforced frame really depended upon the order of the loading. This was a very complex problem. In order to get some insight the following analyses were performed. The OP load to failure was determined for a single bay CMU and brick infill

frame. The load was applied as a distributed pressure on the infill. The ultimate loads are given in Table 3. For the CMU, $P_{u\text{-}out}$ = 38.6 kN and for the brick, $P_{u\text{-}out}$ = 57.4 kN. They are very much less than the IP ultimate loads. The in-plane ultimate for the CMU, $P_{u\text{-}in}$ = 498 kN, for brick $P_{u\text{-}in}$ = 529 kN. This difference is to be expected due to the very different stiffness in the direction being loaded. For the IP load, the structure appeared as a very deep, short beam and could take a great load. For the OP load, the problem looked like a reinforced plate. The bending stiffness would be proportional to the thickness cubed. Clearly the relevant thickness was very different in each case and lead to the different ultimate loads. At the ultimate load, the columns have failed half way through the thickness and about ¼ the way up the column. None of the CMU or brick had broken. The brick infill frame seemed to have failed a little further into the column thickness than for the CMU infill frame. The brick infill frame had the higher ultimate strength because the strength of the brick was greater than the CMU strength. The overall stiffness of the structures was similar by the measure used here. This indicated the out-of-plane stiffness was mostly determined by the frame and not so much by the infill.

Out-of-plane and in-plane loading - Without a specific loading in mind, combining in-plane and out-of-plane loading is problematic because of the path-dependent nature of the problem. For example, during a seismic event the actual load may be applied at some angle and change with time. The combined loading case is a simplified try at seeing how the in-plane and out-of-plane loads interact.

For this investigation, ½ the OP load to cause failure was applied and then the IP load increased until failure was registered. Note that for the problems at hand this led to a very different path of loading between the CMU and brick cases. For the CMU infill case, ½ the OP load was still elastic, i.e. none of the material has failed. For the brick infill case, ½ the OP load was in the inelastic region, i.e. some of the material had failed. The question was: does an elastic pre-load produce the same type of effect as a pre load that caused flaws to develop? Probably not, but this is outside the scope of the work here.

A conclusion was made: out-of-plane loading significantly reduced in-plane strength. Current analytical practices neglect the effects of out-of-plane loading on the in-plane strength.

Comparison between Joint Distributed and End Concentrated Loading at Story Levels

To compare the experimental response of a model loaded only at one end with more distributed loading that would occur in a building in an earthquake, a different type of in-plane loading was analyzed. It was a more distributed type of loading, DIP. The load was applied as a volumetric load at the beam-column intersection. The displacements used in the following load deflection curves were averaged at the elements in the intersection region. This type of load appeared to be more like a seismic load and was very different than the in-plane loading previously used. It was first used in a triple bay/story CMU and a triple bay/story brick frame structure. The structure appeared to be much stiffer with respect to the DIP load than the CIP load. Examining the corresponding failed material maps revealed there is more failed mortar when the load is distributed, leading to the more ductile behavior. Overall the structure was much stiffer

when the load was concentrated at the beam ends. For this case the frame behaved like a very deep, stiff beam. When the load was distributed, the structure performed more like a parallel set of beams, none of which were as strong as the structure loaded on the end. The importance in these results pertained to how seismic loads are simulated statically.

DIP type loading resulted in a 15% increase over the CIP loading for the CMU infilled frame. However, in the case of the brick infill, a decrease in strength of 10% was observed. It was expected that both CMU and brick would have an increase in strength under DIP loading. The decrease in strength in the case of the brick was attributed to the load distribution in the non-linear zone. However, it is concluded that the way the load was applied on the models had a significant effect on the order of 15% increase or decrease in load capacity. More study is needed to address the effect of load application type on story levels on the in-plane strength.

SUMMARY, CONCLUSIONS, AND DISCUSSION

1. Considering the complexity of the models and the variations in their material properties, experimental and analytical models agreed fairly within 20% accuracy.
2. Scaling of bare and infilled models by half cannot be satisfied unless the added masses on the half-scale models increase their capacities about 4 times capacity of their full-scale models.
3. The finite element analyses in this study about bay-multiplicity have agreed with the experimental results that concluded that variation in strength of any infill frame per bay is highly nonlinear.
4. The behavior of the models was very sensitive to mortar properties. The precise value greatly affected the structural stiffness and the ultimate load. One would suspect that the change in the weakest property would have had the greatest effect on the ultimate load, and that property was the mortar.
5. Out-of-plane forces significantly reduced in-plane capacity of masonry infilled frames. A combined out-of-plane and in-plane load reduced the in-plane load capacity compared to only an in-plane load.

REFERENCES

Al-Chaar, Ghassan. “Non-Ductile Behavior of Reinforced Concrete Frames with Masonry Infill Panels Subjected to In-Plane Loading.” USACERL Technical Manuscript, 99/18, December 1998.

ANSYS Release 5.5.1, ANSYS, Inc., 275 Technology Drive, Canonsburg, PA 15317, October 1998.

Table 2. Mechanical Properties of Materials

Test		Model 1	Model 2	Model 3	Model 4	Model 5	ASTM	Finite Element
Concrete Compressive Strength	Compressive Strength psi (kPa)	5548 (38226)	6195 (42684)	6195 (42684)	5478 (37743)	4943 (34057)	C39-94	5575 (38412)
Mortar Compressive Strength (N)	Compressive Strength psi (kPa)	N/A	962 (6628)	1058 (7290)	1248 (8599)	1532* (10555)	C109	1343 (9253)
Mortar Compressive Strength (M)	Compressive Strength psi (kPa)							2684 (18493)
CMU Compressive Strength	Gross Compressive Strength psi (kPa)	1872 (12898)	1872 (12898)	1872 (12898)	1872 (12898)	N/A	C140	
	Net Compressive Strength psi (kPa)	2505 (17259)	2505 (17259)	2505 (17259)	2505 (17259)	N/A	C67	2505 (17259)
CMU Prism	Gross Compressive Strength psi (kPa)	2409 (16598)	2409 (16598)	2409 (16598)	1525 (10507)	N/A	E447-84	
	Net Compressive Strength psi (kPa)	3224 (22213)	3224 (22213)	3224 (22213)	2041 (14062)	N/A		
Clay brick Prism	Gross Compressive Strength psi (kPa)	2697 (18582)	2697 (18582)	2697 (18582)	N/A	3555 (24494)	E447-84	
	Net Compressive Strength psi (kPa)	3387 (23336)	3387 (23336)	3387 (23336)	N/A	4369 (30102)		
Brick Compressive Strength	Gross Compressive Strength psi (kPa)	11,743 (80909)	11,743 (80909)	11,743 (80909)	N/A	12,368 (85216)	C140	
	Net Compressive Strength psi (kPa)	14,791 (101910)	14,791 (101910)	14,791 (101910)	N/A	15,202 (104742)	C67	2800 (19292)
#3 Steel Rebar	Elastic Modulus ksi (MPa)	28,300 (194987)	28,300 (194987)	28,300 (194987)	28,300 (194987)	28,300 (194987)	A615-95b	
	Yield Strength ksi (MPa)	49.1 (338)	49.1 (338)	49.1 (338)	49.1 (338)	49.1 (338)	E8-95a	
	Tensile Strength ksi (MPa)	79.0 (544)	79.0 (544)	79.0 (544)	79.0 (544)	79.0 (544)		

*Average of three frames

Table 3. Summary of Models Studied and Load Capacities and corresponding Deflections.

	Mod	Inf	Bay	Stry	Scl	Mrtr	Exp. Load lbs (kN)	Load lbs (kN)	Load Type	O/P lbs (kN)	Deflect. in (cm)
L	01	0	1	1	H	N	6500 (28.9)	6,175 (27.5)	CIP		.44 (1.12)
A	02	C	1	1	H	N	18900 (84.1)	30,000 * (23000)**(133) (102)	CIP		.040 (.102)
B	03	B	1	1	H	N	20000 (89.0)	32,000 * (24000)**(142) (107)	CIP		.044 (.112)
	04	0	2	1	H	N		9,000 (40.0)	CIP		.36 (.91)
	05	C	2	1	H	N	71400 (31.8)	66,000 (294)	CIP		.040 (.102)
	06	0	3	1	H	N		12,250 (54.5)	CIP		.31 (.79)
	07	B	3	1	H	N	83000 (37.9)	67,000 (298)	CIP		.044 (.112)
F	08	0	1	1	F	N		22,400 (99.6)	CIP		.57 (1.45)
U	09	C	1	1	F	N		112,000 (498)	CIP		.045 (.114)
L	10	B	1	1	F	N		119,000 (529)	CIP		.0495 (.1257)
S	11	0	2	1	F	N		37,500 (167)	CIP		.94 (2.39)
C	12	C	2	1	F	N		240,000 (1068)	CIP		.074 (.188)
L	13	O	3	1	F	N		55,000 (245)	CIP		1.35 (3.43)
	14	B	3	1	F	N		240,000 (1068)	CIP		.078 (.198)
3	15	0	3	3	F	N		29,400 (130)	CIP		
S	L1										.0025 (.0064)
T	L2										.0050 (.0127)
O	L3										.0057 (.0145)
R	16	C	3	3	F	N		249,000 (1108)	CIP		
I	L1										.000273 (.000693)
S	L2										.000408 (.001036)
	L3										.000552 (.001402)
	17	B	3	3	F	N		252,000 (1121)	CIP		
	L1										.000519 (.001318)
	L2										.000787 (.001999)
	L3										.00104 (.00264)
	18	C	3	3	H	M		276,000 (1128)	CIP		
	19	B	3	3	H	M		288,000 (1281)	CIP		
O	20	C	1	1	F	N			OP	8,700 (38.6)	
+	21	C	1	1	F	N		93,500 (416)	½OP/CIP	4,350 (19.3)	
I	22	B	1	1	F	N			OP	12,900 (57.4)	
	23	B	1	1	F	N		94,000 (418)	½OP/CIP	6,450 (28.7)	
	24	C	3	3	H	N		286,800 (1276)	DIP		
	25	B	3	3	H	N		225,600 (1003)	DIP		

* For shear retention values $\beta c = 0.6$ and $\beta t = 0.3$ ** For shear retention values $\beta c = \beta t = 0.005$

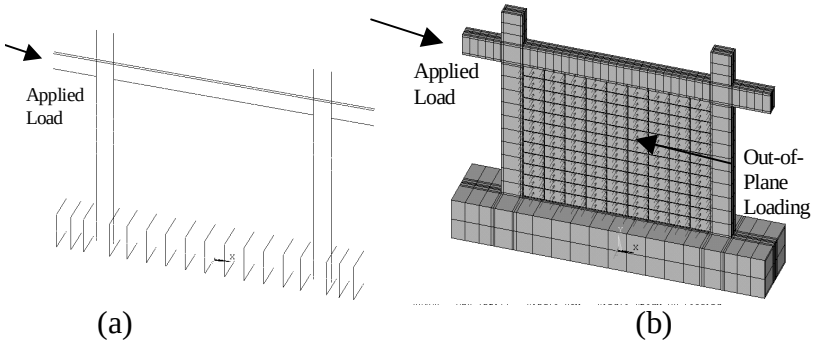

Figure 1. Single-Bay, Single-Story Models. (a) Reinforcement Detailing, (b) Application of Concentrated In-Plane and Out-of-Plane Loading.

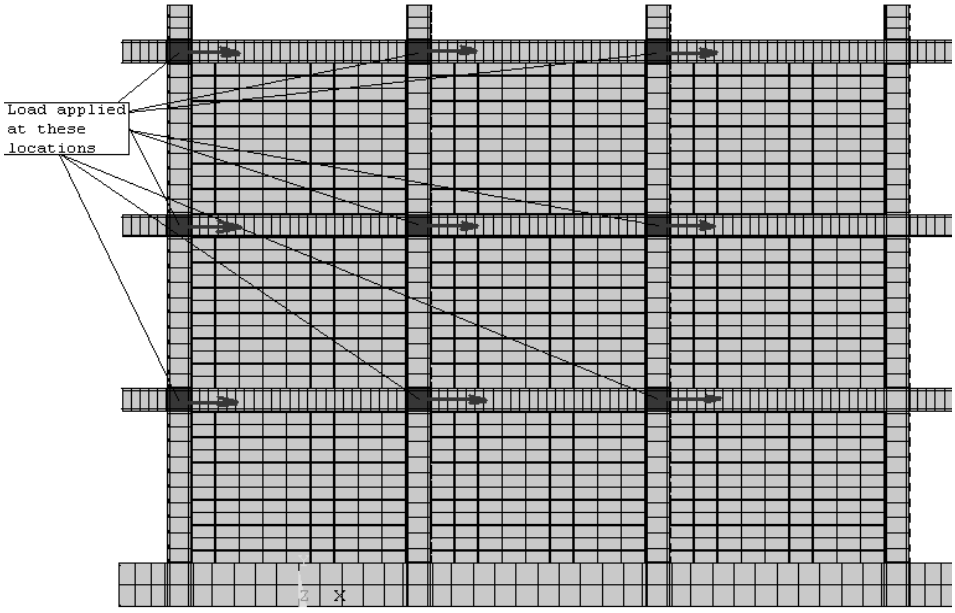

Figure 2. Force Application for Triple-story models.

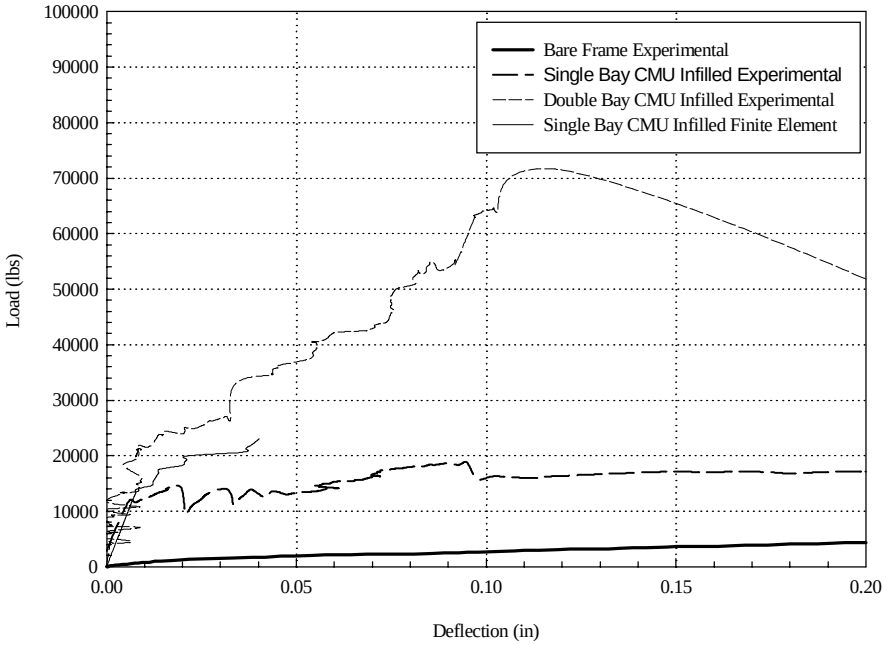

(1 lb = 4.448 N, 1 in = 2.54 cm)

Figure 3: Single Story, Half-Scale CMU Infilled Models, Experimental and Finite Element Analysis

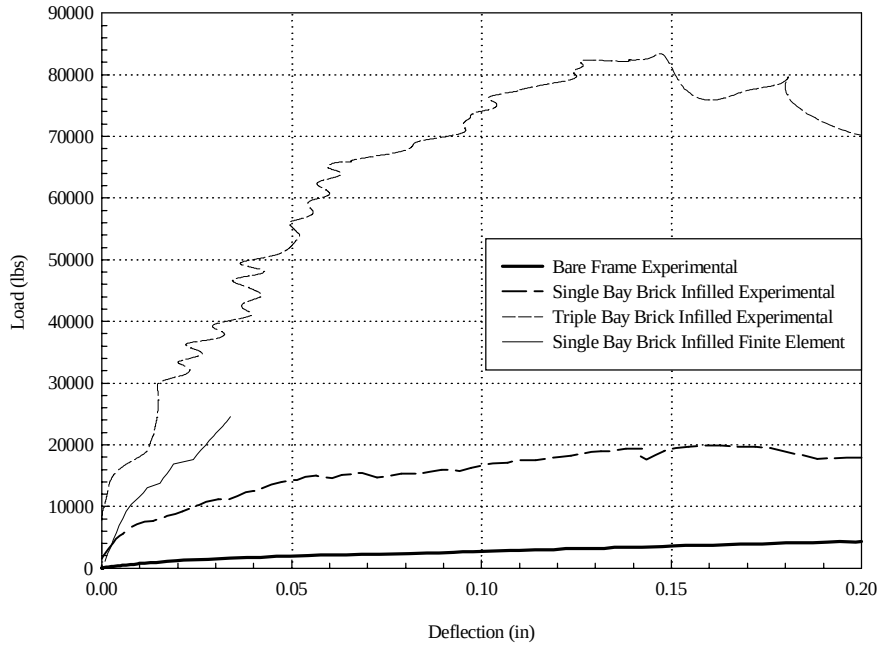

(1 lb = 4.448 N, 1 in = 2.54 cm)

Figure 4: Single Story, Half-Scale Brick Infilled Models, Experimental and Finite Element Analysis